

Radiative recombination from InP quantum dots on (100) GaP

F. Hatami^{a)} and W. T. Masselink

Department of Physics, Humboldt-Universität zu Berlin, Invalidenstrasse 110, D-10115 Berlin, Germany

L. Schrottke

Paul-Drude-Institut, Hausvogteiplatz 5-7, D-10117 Berlin, Germany

(Received 5 June 2000; accepted for publication 13 February 2001)

We describe the growth and optical emission from strained InP quantum dots grown on GaP using gas-source molecular beam epitaxy. Self-organized island formation takes place for InP coverage greater than 1.8 monolayers on the (100) GaP surface. Intense photoluminescence from the dots is peaked at about 2.0 eV, blueshifted by 0.6 eV from the band gap of bulk InP due to strain, quantum size effects, and possibly Ga interdiffusion. © 2001 American Institute of Physics.

[DOI: 10.1063/1.1361277]

Self-organization during growth is the prevalent method for the formation of quantum dots (QDs), structures which are not only inherently important for the understanding of quasizero-dimensional quantum systems, but also offer promising improvements in optical devices.¹ In particular, quantum dots allow further freedom in controlling the emission wavelength than do quantum wells; for example, InAs quantum dots in a GaAs matrix have recently allowed the fabrication of 1.3 μm lasers on GaAs substrates.²

Analogous to the InAs/GaAs system, QD formation of InP on GaP due to the Stranski–Krastanov mechanism is expected under the proper growth conditions, driven by the 7.7% lattice mismatch between InP and GaP.³ Optical emission from these direct-band gap InP islands embedded in the indirect GaP matrix is expected to lie between the InP and GaP band gaps. In the related materials system, InP/In_{0.48}Ga_{0.52}P, intense photoluminescence (PL) due to radiative recombination of heavy holes and electrons in the InP QDs embedded in In_{0.48}Ga_{0.52}P is observed at energies between 1.6 and 1.85 eV.⁴ The use of GaP as the substrate has further potential advantages of larger strain and larger band gap difference, allowing more flexibility in varying the emission wavelength. Additionally, structures on GaP could take advantage of well-developed light-emitting diode (LED) technology. Furthermore, using GaP rather than GaAs as the substrate allows easier extraction of the emitted light for vertical structures including vertical cavity lasers.

In the present work we describe for the first time, we believe, the optical emission from InP QDs embedded in a (100)-oriented GaP matrix. Structural analysis indicates that the dots are approximately $100 \times 100 \text{ nm}^2$ in lateral extent and about 20 nm high. Photoluminescence measured between 5 and 300 K is characterized by an intense peak centered at about 2.0 eV, following approximately the temperature dependence of the InP band gap, but shifted 0.6 eV higher in energy.

Structures were grown by gas-source molecular beam epitaxy (GSMBE) on GaP(100) substrates using a Riber-32-P MBE system. Prior to growth, the substrates were etched in a solution of 4HCl:4HNO₃:5H₂O.⁵ After oxide de-

sorption, a 200 nm thick GaP buffer layer was grown at 565 °C at a rate of 2 $\mu\text{m}/\text{h}$. The growth was then interrupted while the substrate temperature was reduced. Subsequently, the desired coverage of InP was deposited at 490 °C, followed by a growth interruption of 60 s. The resulting structures were then capped with GaP. The structures grown for PL measurements contain three to five identical InP layers, each with thickness between 0.5 and 5.8 monolayers (MLs) separated by 5–20 nm of epitaxial GaP. (We measure the InP coverage in monolayers on the GaP surface; 1 ML = 6.7×10^{14} In atoms cm^{-2} .) The growth process was monitored by the reflection high-energy electron diffraction (RHEED) patterns; during GaP growth, the surface showed (2×4) reconstruction. At the beginning of InP growth, the RHEED pattern appeared streaky, indicating two-dimensional (2D) growth, and gradually became spotty and less intense after deposition of about 1.8 ML of InP (3D growth). The samples used for atomic force microscopy (AFM) studies were grown without the cap layer.

AFM investigations of the uncapped structures were carried out in a TopoMetrix Discover microscope. Both the *in situ* RHEED measurements and the AFM studies indicate that island formation begins after deposition of about 1.8 ML of InP. Figure 1 shows an AFM image of a sample with nominally 5.8 ML of InP. Similar AFM investigations of samples with different InP coverage indicate that (1) all have a relatively large distribution of the dot base size (typical standard deviation of 40 nm) with an average base length between 100 and 120 nm; (2) the dot height increases with increasing base length, being about 20 nm for 100 nm base length dots; (3) the dot density scales with the amount of InP deposited and is in the range of $2\text{--}6 \times 10^8 \text{ cm}^{-2}$ for samples with InP coverage between 1.9 and 5.8 ML. The amount of InP contained in the wetting layer (whose thickness is determined from both the onset of QD formation and from PL measurements) and in the QDs, determined by their dimensions and densities measured using AFM, is consistent with the total amount of InP deposited.

These dots are significantly larger than those typically observed in other systems with large lattice mismatch. Island size depends on a variety of factors including the specific properties of the material system and the growth conditions.

^{a)}Electronic mail: hatami@physik.hu-berlin.de

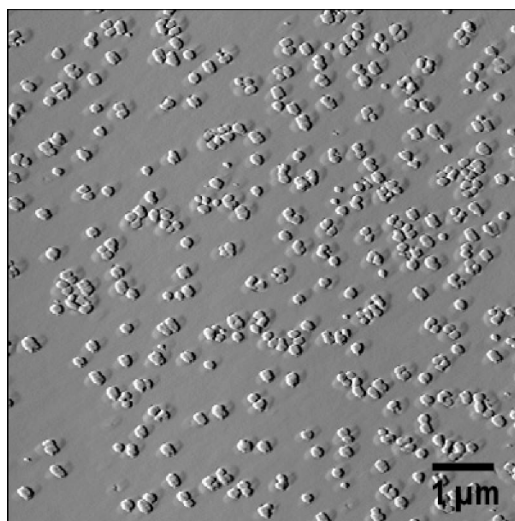


FIG. 1. Atomic force micrograph of InP quantum dots with 5.8 ML InP coverage on a (100) GaP surface.

According to our observations, higher phosphorus flux leads to smaller islands. The same effect has also been reported in the InAs/GaAs system,⁶ which also resulted in QDs as large as 100 nm. Higher magnification AFM images indicate that the larger islands in our distributions are probably composed of two to four smaller dots which have grown together; a detailed statistical analysis shows no indication, however, of a multimodal size distribution. Further investigations regarding the growth itself are underway and this letter will focus on the optical properties of QDs.

Photoluminescence measured in the range of 5–300 K is excited using the 325 nm line of a He–Cd laser. The emission is dispersed using a monochromator and detected using a charge coupled device (CCD) camera. Figure 2 shows the PL spectra of three InP/GaP structures, one containing a strained 2D InP layer (sample A) and the others with QDs (samples B and C). The InP in the first structure remains 2D because the 0.5 ML of InP coverage is considerably lower than the critical thickness for island formation; the InP coverage in the structures containing QDs, however, is above this critical thickness. For comparison, the luminescence from the epitaxial GaP buffer is also shown. The InP/GaP samples consist of five periods containing 0.5 ML (2D sample), 1.9 ML (QD sample B), and 2.3 ML InP (QD

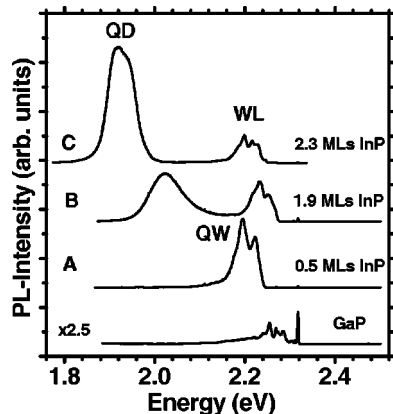


FIG. 2. Photoluminescence spectra of samples with different InP coverage measured at 5 K.

sample C), respectively. The InP growth rate was about 0.08 $\mu\text{m}/\text{h}$ for sample B and 0.22 $\mu\text{m}/\text{h}$ for samples A and C. The measurements were carried out at 5 K with an excitation energy of about 20 W cm^{-2} .

The PL emission from the 2D InP sample consists of two intense relatively narrow PL lines separated by 30 meV. These lines in the 2.15–2.20 eV range appear to result from electron-hole recombination in the strained InP quantum well and appear to be similar to emission from strained GaAs quantum wells on GaP.⁷ For InP coverage greater than 1.8 ML, both RHEED and AFM indicate three-dimensional growth resulting in the quantum dots. The PL from such samples includes additional emission at about 2.0 eV and is attributed to radiative recombination of heavy holes and electrons in the dots. The reason for the redshift of the QD luminescence in sample C compared to that in sample B is the higher InP coverage in sample C. The AFM data also indicate that increased InP coverage results in larger dots. The PL associated with the 2D InP wetting layer remains, but is shifted towards higher energy and is weaker. These effects resemble those of the InAs/GaAs system and indicate that a part of the wetting layer is consumed in the formation of the QDs.⁸

To analyze the QD emission we calculate the band alignment between the InP QDs and the GaP matrix. Because the lateral dimensions for the QDs are much larger than their vertical dimensions, we neglect the lateral confinement effects and model the QDs as quantum wells with thickness of 20 nm. The band alignment between the InP QW layer and the GaP, including strain effects, is estimated using the model-solid theory of Van de Walle.⁹ The localization energies for both electrons and heavy holes are calculated as functions of InP thickness. Within this simple, multivalley effective-mass approximation, we find that for the InP/GaP heterostructures with InP thickness thinner than about 3 nm, the Γ -like electrons in the InP layer are located at a higher energy than X states in the GaP layer and the structure is type II. Since the wetting layer is always thinner than 3 nm [the 2D to three-dimensional (3D) transition takes place at 1.8 ML \approx 0.6 nm], these 2D InP films in GaP are expected to always be type II. Our model indicates that in the QDs, on the other hand, the Γ -like electrons in the InP QDs are located at approximately the same energy as the X valley in the GaP matrix, resulting in the electrons being in both materials. For this reason, the electrons in both InP and GaP layer are similarly available for carrier recombination, and the band alignment for InP QDs embedded in a GaP matrix is near the transition between type I and type II. Figure 3 shows the corresponding band alignment. A similar treatment was successfully used in interpreting the results of InP QDs in $\text{In}_{0.48}\text{Ga}_{0.52}\text{P}$, where luminescence is observed in the energy range of 1.60–1.85 eV.⁴ The luminescence from InP QDs on GaP is higher in energy due to the greater strain and greater band gap difference compared to $\text{InP}/\text{In}_{0.48}\text{Ga}_{0.52}\text{P}$. The blueshift from the InP band gap of 0.61 eV can also be compared to the blueshift in the InAs/GaAs system of over 0.8 eV.

We explain the double peak luminescence from the 2D InP as the spatially indirect recombination of electrons from the GaP X valleys with holes in the InP and its phonon replica involving the longitudinal acoustic (LA) phonon near

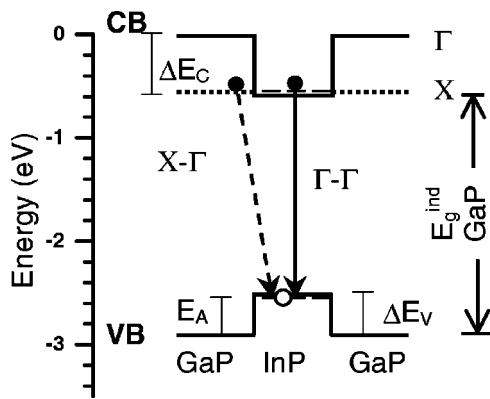


FIG. 3. Valence and conduction band alignment schematic of InP QDs embedded in the GaP matrix. The arrows indicate both possibilities of electron-hole recombination.

the X points in the Brillouin zone.¹⁰ The energetic separation of 30 meV remains constant even as the luminescence from the 2D InP shifts towards higher energy in samples which also contain QDs, supporting identification of the lower energy of the two as a phonon replica. The third peak in the PL from the 2D InP in sample C, lying between the main recombination peak and the one associated with the LA phonon, may be due to transverse acoustic (TA) phonons, also near the X points.

Figure 4 shows the temperature evolution of the PL from sample C with 2.3 ML of InP coverage. As the temperature is increased from 5 K, the luminescence shifts from the wetting layer to the QDs (with increased QD luminescence) due to the interplay between various capture and recombination channels. This behavior is similar to what we observe in the InAs/GaAs system and what is also seen in the GaSb/GaAs

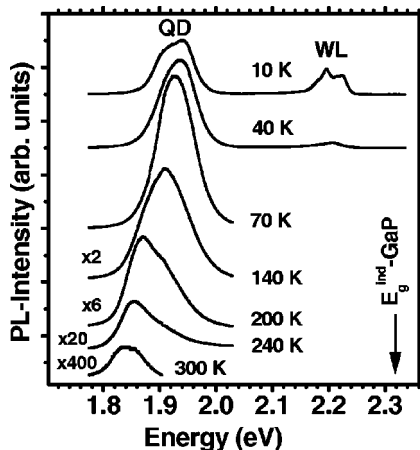


FIG. 4. Temperature dependence of the PL spectra of sample C with InP QDs resulting from 2.3 ML InP coverage.

system.¹¹ At higher temperatures, the overall luminescence intensity decreases, typical of undoped semiconductors. The temperature dependence of the InP QD emission energy is typical of III–V semiconductors;¹² we are not, however, able to distinguish whether it follows the temperature dependence of bulk InP or GaP better. We have analyzed the integrated PL intensity from the QDs as a function of temperature and obtain an activation energy of 398 ± 20 meV which corresponds to the energy difference between the QD luminescence and the GaP indirect band gap. This result agrees with our band alignment modeling and indicates that the Γ valley in the InP QDs is aligned approximately with the X valley in the GaP matrix and that the observed thermal activation is that of the holes leaving the QDs (see Fig. 3).

To conclude, we have demonstrated the growth of InP QDs on (100) GaP. The QDs appear to form via the Stranski–Krastanov mechanism after a critical InP coverage of 1.8 ML is reached. When the InP dots are overgrown with GaP, intense PL from the InP QDs peaked at 2.0 eV is observed. This energy is 0.6 eV higher than the bulk InP band gap due to strain, quantum confinement, and probably also Ga interdiffusion. Thicker InP coverage leads to slightly larger dots and somewhat lower energy luminescence. This luminescence persists to above room temperature, but decreases due to the holes being thermally excited out of the QDs. The potential for applications as a light emitter in this energy range, but with higher efficiency than that of the currently used systems, is promising.

The authors thank K. Braune for AFM measurements.

¹ Y. Arakawa and H. Sakaki, *Appl. Phys. Lett.* **40**, 939 (1982).

² D. L. Huffaker, G. Park, Z. Zou, O. B. Shchekin, and D. G. Deppe, *Appl. Phys. Lett.* **73**, 2564 (1998).

³ B. Junno, T. Junno, M. S. Miller, and L. Samuelson, *Appl. Phys. Lett.* **72**, 954 (1998).

⁴ F. Hatami, U. Müller, H. Kissel, K. Braune, R.-P. Blum, S. Rogaschewski, H. Niehus, H. Kirmse, W. Neumann, M. Schmidbauer, R. Köhler, and W. T. Masselink, *J. Cryst. Growth* **216**, 26 (2000).

⁵ J. N. Baillargeon, K. C. Hsieh, and G. E. Stillman, *J. Appl. Phys.* **68**, 2133 (1990).

⁶ N. N. Ledentsov, M. Grundmann, N. Kirstaedter, O. Schmidt, R. Heitz, J. Böhrer, D. Bimberg, V. M. Ustinov, V. A. Shchukin, A. Yu. Egorov, A. E. Zhukov, S. Zaitsev, P. S. Kopev, Zh. I. Alferov, S. Ruvimov, P. Werner, U. Gösele, and J. Heydenreich, *Solid-State Electron.* **40**, 785 (1996).

⁷ J. A. Prieto, G. Armelles, M.-E. Pistol, P. Castrillo, J. P. Silveira, and F. Briones, *Appl. Phys. Lett.* **70**, 3449 (1997).

⁸ T. R. Ramachandran, R. Heitz, P. Chen, and A. Madhukar, *Appl. Phys. Lett.* **70**, 640 (1997).

⁹ C. Van de Walle, *Phys. Rev. B* **39**, 1871 (1989).

¹⁰ M.-E. Pistol, M. Leys, and L. Samuelson, *Phys. Rev. B* **37**, 4664 (1988).

¹¹ F. Hatami, N. N. Ledentsov, M. Grundmann, J. Böhrer, F. Heinrichsdorff, M. Beer, D. Bimberg, S. Ruvimov, P. Werner, U. Gösele, J. Heydenreich, U. Richter, V. Ivanov, B. Ya. Meltser, P. S. Kopev, and Zh. I. Alferov, *Appl. Phys. Lett.* **67**, 656 (1995).

¹² Y. P. Varshni, *Physica (Amsterdam)* **34**, 149 (1967).